Testing of electron beam irradiated sheep wool for adsorption of Cr(III) and Co(II) of higher concentrations

Jana Braniša [a], Klaudia Jomová [a], Ľubomír Lapčík [b,c], Mária Porubská [a,*]

[a] *Department of Chemistry, Faculty of Natural Sciences, Constantine the Philosopher University in Nitra, Tr. A. Hlinku 1, 949 74, Nitra, Slovakia*
[b] *Regional Centre of Advanced Technologies and Materials, Department of Physical Chemistry, Faculty of Science, Palacky University, 17. Listopadu 12, 771 46, Olomouc, Czech Republic*
[c] *Tomas Bata University in Zlin, Faculty of Technology, Nam. T.G. Masaryka 275, 760 01, Zlin, Czech Republic*

ARTICLE INFO

ABSTRACT

Electron beam irradiated sheep wool dosed (0–410) kGy showing good adsorption properties was tested for Cr (III) and Co(II) of higher concentrations. Fitting to ten isotherm models was examined as follows: Langmuir, Freundlich, Dubinin-Radushkevich, Temkin, Flory-Huggins, Halsey, Harkins-Jura, Jovanovic, Elovich and Redlich-Peterson. Both cations being Lewis acids generate complex salts, such as carboxylates or cysteinates, with ligands from keratin. Various composition and architecture of the complexes are responsible for different isotherm model fitting. The chromic cation showed adherence to Freundlich, Temkin, Halsey, Harkins-Jura and Jovanovic models for all or almost all dosed samples unlike cobaltous cation matching Langmuir, Flory-Huggins and Redlich-Peterson isotherm models. No model fitted the both examined cations simultaneously. On the contrary, simultaneously non-fitting to all dosed samples was observed for Elovich and partially Dubinin-Radushkevich models.

1. Introduction

Although adsorption processes have long been a part of various technological processes, their current importance increases the interest in the circular economy in the recovery of valuable materials. An important application of adsorption processes is also in the protection of the environment in the removal of unwanted components of waste water [1,2]. The phenomenological approach to adsorption led to the development of a mathematical apparatus for adequate description in the form of various models of mostly empirical character. These models were applied to adsorbents of inorganic origin [3], biosorbents native [4] or modified [5], biochars [6] and synthetized materials [7]. The aim of the published studies was to find the best fitting model for the adsorbent - adsorbate system used. The correlation coefficient R^2 of linearized model equations was considered to be a fit criterion and, adsorption parameters were calculated from the equations. It is expected that an acceptable match may be indicated for $R^2 \geq 0.9$, the more the correlation coefficient is closer to one. To facilitate comparisons, some papers also present even lower R^2 values [7,8] and they also declare the corresponding calculated parameters. It is worth to note that the studies published so far only dealt with adsorbate concentrations below of 10

mmol .dm^{-3}. A possible reason is that at higher concentrations the sorption efficiency decreases substantially and the reasoning is not always easy. Increasing the adsorbate concentration may lead to a change in the mechanism of the sorption process and thus a change in the corresponding isotherm model.

Given the current surplus of waste sheep wool, it is somewhat surprising that a modest number of works has been published on native wool as adsorbent, although the composition of wool keratin provides good prospects for this [9]. Among the few, one can find the work of Ghafar et al. [10], who treated the wool with citric acid. The pulverized raw (PW) and the treated wool (MPW) were pulverized and used to remove Methylene Blue from an aqueous solution. The adsorption equilibrium of both was examined applying Langmuir, Freundlich and Dubinin-Radushkevich models. Langmuir's model for PW indicated R^2 = 0.7332 and for MWP 0.8878, resp. Freundlich's model for PW attained R^2 = 0.955 and for MWP 0.936, resp., while Dubinin-Radushkevich's model for PW showed R^2 = 0.962 and for MPW 0.95 resp., indicating probably chemisorption.

So far insufficiently investigated adsorbent has been sheep wool irradiated with accelerated electron beam examined by Porubská et al. [11]. The electron beam penetrates the entire fiber volume and

---

* Corresponding author.
E-mail addresses: jbranisa@ukf.sk (J. Braniša), kjomova@ukf.sk (K. Jomová), lapcikl@seznam.cz (Ľ. Lapčík), mporubska@ukf.sk (M. Porubská).

Table 1

The conditions of calculation and plotting curves to test fit of examined isotherm models.

No.	Isothem model	Units used for calculation	Plot of dependence
		$(C_0, C_e; q_e; \Theta)$	
1	Langmuir	mg.dm^{-3}; mg.g^{-1}	C_e against C_e/q_e
2	Freundlich	mg.dm^{-3}; mg.g^{-1}	$log\ C_e$ against $log\ q_e$
3	Dubinin-Radushkevich	mg.dm^{-3}; mg.g^{-1}	$\mathcal{E}^2$ against $ln\ q_e$
4	Temkin	mg.dm^{-3}; mg.g^{-1}	$ln\ C_e$ against q_e
5	Flory-Huggins	mol.dm^{-3}; mol.g^{-1}	$log\ (1-\Theta)$ against $log\ (\Theta/C_0)$
6	Halsey	mg.dm^{-3}; mg.g^{-1}	$ln\ c_e$ against $ln\ q_e$
7	Harkins-Jura	mg.dm^{-3}; mg.g^{-1}	$log\ C_e$ against $1/q_e^2$
8	Jovanovic	mg.dm^{-3}; mg.g^{-1}	C_e against $ln\ q_e$
9	Elovich	mg.dm^{-3}; mg.g^{-1}	q_e against $ln\ (q_e/C_e)$
10	Redlich-Peterson	mg.dm^{-3}; mg.g^{-1}	$ln\ C_e$ against $ln\ (C_e/q_e)$

Note: Meaning of basic symbols: C_e is concentration of adsorbate at equilibrium, q_e is amount of adsorbate adsorbed at equilibrium, C_0 is adsorbate initial concentration, Θ is degree of surface coverage.

considerably affects its primary and secondary structure. Cleavage of the disulfide bonds and subsequent oxidation reactions of the radicals lead to the generation of cystine oxides and cysteic acid. Thus, in addition to the original carboxyl groups of keratin, the number of acidic functional groups for chemical interaction with adsorbate is available. So far the published studies describe the adsorption of Cu (II) [12], Co(II) and Cr (III) [13,14] on such wool with a different absorbed dose of energy.

The elements chromium and cobalt belong to the elements of 4th period of the periodic table as the first series of transition elements (3d-elements). Their valence orbital configuration is [Ar]$3d^5 4s^1$ for Cr and [Ar]$3d^7 4s^2$ for Co and, that is why they tend to form complexes. Keratin containing various functional groups, including amine/imine or hydroxyl, provides good complexing conditions. All chromium complexes without exception have a coordination number of 6 and an octahedral form [15]. In the case of Co, a coordination number of 4 or 6 with a tetrahedral or octahedral structure are customary.

The aim of this work is to search for an isotherm model acceptably describing the process of adsorption of Co(II) and Cr(III) from aqueous solutions without any pH adjustment and in higher concentrations in the range of 10–200 mmol dm^{-3} on sheep wool both native and electron beam irradiated with various absorbed doses. To our knowledge, there is no information of this kind in available scientific resources except recent work of Porubská et al. [16] studying Cu(II) adsorption under comparable conditions. Considering the complicated structure of the native wool itself and even more complicated structure after electron beam modification, we wanted to find out at least some basic initial data relating the modified wool and corresponding isotherm models for adsorption of Co(II) and Cr(III) of higher concentrations.

2. Experimental

Sheep wool came from spring sheep-shearing (2018) of a Merino-Suffolk crossbreed. The wool was scoured using ultrasonic bath, dried and irradiated in UELR–5–1S linear electron accelerator (FGUP NIIEFA, Petersburg, Russia) with installed energy of 5 MeV and operated by Progresa Final SK, Bratislava. The samples with absorbed doses of (0–21–40–99–153–258–410) kGy were stored under common conditions and room temperature and used for sorption batch experiments.

Chemicals chromium potassium sulphate dodecahydrate KCr (SO$_4$)$_2$·12H$_2$O p.a., supplied by Gavax, Ltd., (Vranov n/Topl'ou, Slovakia) was used as Cr(III)-adsorbate. Cobalt dichloride hexahydrate CoCl$_2$.6H$_2$O p.a. was provided from Centralchem (Bratislava, Slovakia). Stock solutions of both Cr(III) and Co(II) salts were prepared by dissolving appropriate amount of the mentioned salts in deionized water and diluting to desired initial concentrations. The applied

concentrations were of (12.5–25–50–60–70) mmol.dm^{-3} for Cr(III) and (50–100–125–150–200) mmol.dm^{-3} for Co(II). The use of the concentrations was motivated by the absence of adsorption data for higher amounts using any other adsorbents as well as the tendency of these elements to form complex salts provided their sufficient concentration. At the same time, such concentrations allow analysis by UV-VIS spectrometry.

Visible spectrometry (Specord 50 Plus, Analytikjena, Germany) with 1 cm cell was used to determine of Cr(III) ($\lambda = 583$ nm) or Co(II) ($\lambda = 512$ nm) content in the bath. The comparative sample was always the aqueous extract from the wool with dose corresponding to the measured sample, obtained after 24 h contact of the sample with deionized water under the same conditions.

The batch sorption experiments were conducted with Cr(III) or Co(II) solutions applying corresponding above mentioned concentrations. After being cut to 3–5 mm, 0.2 g of wool fibres was placed into a glass cup with a cap and the testing solution of 20 cm^3 in volume was added. The content of the glass cup was shaken for first 6 h at room temperature on a laboratory horizontal shaker (Witeg SHR–2D, Labortechnik GmbH, Wertheim, Germany) and then kept in static mode for next 18 h. Then the remaining solution was filtered through KA5 filter paper and used for determination of residual Cr(III) or Co(II). Every sorption procedure was carried out in triplicate.

The parameter q_e as a measure of wool sorptivity at equilibrium was calculated using the following Equation (1):

$$q_e = (x_1 - x_2)/m \qquad (1)$$

where q_e is the sorptivity defined as the equilibrium amount of sorbate in mmol per 1 g of the sorbent for individual wool samples when particular testing solution is applied in specified concentration.

x_1 is the amount of the sorbate added in the initial solution (mmol),
x_2 is residual equilibrium amount of the sorbate in the solution after its contact with the wool sample (mmol),
m is the mass of wool sample taken for analysis (g).

Scanning Electron Microscopy (SEM) images of the wool fibers were taken by scanning electron microscope (SEM) Hitachi 6600 FEG (Japan) operating in the secondary electron mode and using an accelerating voltage of 1 kV.

The isotherm models selected to examine whether they match the measured data are summarized in Table 1. The data needed to calculate the parameters of the individual isotherm models were obtained from the graph dependencies generated for each model, cation and absorbed dose using Excel, also providing correlation equations for linearized relationships.

3. Results and discussion

3.1. Adsorption and isotherm models tested

Carboxyl groups are available in wool keratin to form the corresponding salts by ion exchange mechanisms. The cations Cr(III) and Co (II) represent Lewis acids, which readily form complex forms with the available amino, imino and hydroxyl functional groups as ligands. In the irradiated wool, cysteic acid coming from oxidized cleaved S-S bridges [17] adds to the original acidic carboxyl groups, which supports the formation of additional salts and consequently complexes. Therefore, it can be expected that the formation of complexes on the wool surface or bulk will play an important, if not determining role. This is also indicated by the course of sorptivity for Co(II) on the different dosed wool (Fig. 1), which shows atypical fluctuation in the range of applied concentrations. Indeed, the formation of complexes with wool has been proven for both cations [13,14], which presupposes a sufficiently high concentration of the central cation. I our case, the selected range of the
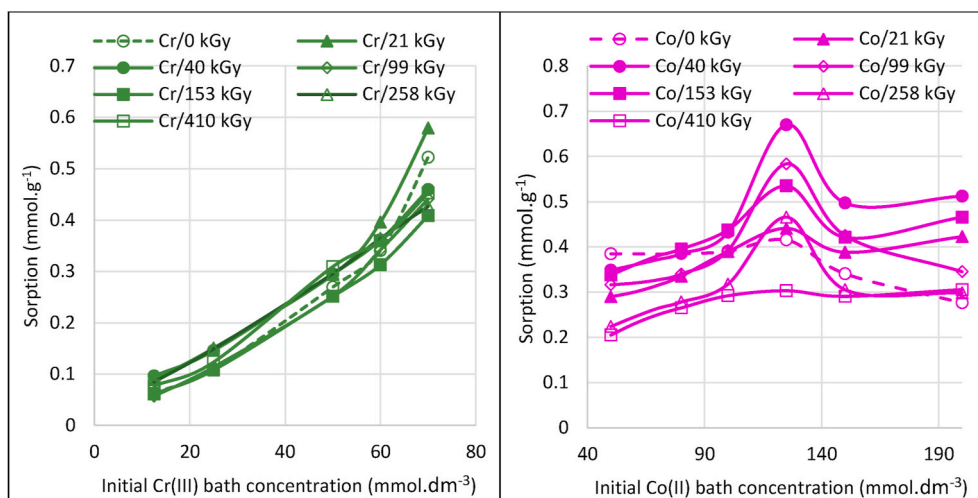
Fig. 1. Sorptivity of Cr(III) and Co(II) on wool native and electron irradiated with various absorbed doses.

Table 2
Overview of the linearized equations of the tested isotherm models.

No.	Model	Linearized equation
1	Langmuir	$\frac{C_e}{q_e} = \frac{1}{Q \cdot K_L} + \frac{1}{Q} C_e$
2	Freundlich	$\log q_e = \log K_F + \frac{1}{n} \cdot \log C_e$
3	Dubinin-Radushkevich	$\ln q_e = \ln q_s - K_D \varepsilon^2; \ \varepsilon = RT \ln\left(1 + \frac{1}{c_e}\right)$
4	Temkin	$q_e = \frac{RT}{b} \ln K_T + \frac{RT}{b} \ln C_e$
5	Flory-Huggins	$\log\left(\frac{\theta}{C_o}\right) = \log K_{FH} + n \log(1 - \theta)$
6	Halsey	$\ln q_e = \frac{1}{n_H} \ln K_H - \frac{1}{n_H} \ln C_{q_e}$
7	Harkins-Jura	$\frac{1}{q_e^2} = \frac{B}{A} - \left(\frac{1}{A}\right) \log C_e$
8	Jovanovic	$\ln q_e = \ln q_{max} - K_J C_e$
9	Elovich	$\ln \frac{q_e}{c_e} = \ln K_E \cdot q_m - \frac{1}{q_m} C_e$
10	Redlich-Peterson	$\ln \frac{C_e}{q_e} = \beta \ln C_e - \ln A$

Note: Meaning of the basic symbols is given in Table 1; the other symbols belong to individual constants or indicators [3,18,19].

adsorbate concentration used in the KCr(SO$_4$)$_2$.12H$_2$O and CoCl$_2$.6H$_2$O bathes was limited by the absorbance for the equilibrium concentration under the VIS spectrometric measurements so that the read absorbance was as accurate as possible and did not exceed value of 1.0.

Fig. 1 shows the effect of absorbed dose on sorptivity. However, to examine each model fitting from the experimental data, the appropriate parameters required to construct the plots were calculated for each isotherm model and each absorbed dose. In this manner, nine one-parameter models were submitted to test as follows: Langmuir, Freundlich, Dubinin-Radushkevich, Temkin, Flory-Huggins, Halsey, Harkins-Jura, Jovanovic, Elovich and one three-parameter Redlich-Peterson. Linearized equations of the models are summarized in Table 2.

The equations of the linear trend lines obtained from the plots are shown in Table 3 involving the fitting and quasi fitting isotherm models only. The non-fitting data can be found in the Appendix.

3.2. Analysis of the model conformity

Knowing the above mentioned isotherm models are mostly empirical relationships, any resulting findings cannot be considered to be true absolutely however, they provide more or less probable information. In addition, sheep wool is a complicated material and the electron irradiation further increases diversity of the structure. Therefore, we assumed that the appearance of the surface of both non-irradiated and irradiated fibers will also be different, affecting the adsorption. As documented by

SEM images (Fig. 2), only minor morphological differences can be observed on the wool surface of unexposed and irradiated with a high dose.

While other published photos of native fiber surface show clear contours of a smooth scare surface [18], the surface of our fiber is a little rougher, with a more rugged topography and has less clear scales contours. We attribute this difference to the scouring method used; the fiber with smooth regular scales [18] was scoured using a standard industrial process, while the fibers used in this study were washed in tap water without chemicals but with ultrasound support [13,14]. It is just the ultrasound effect we attribute a soft erosis of the original surface to.

For a simple classification of the data in Table 3, we predetermined the correlation parameter $R^2 \geq 0.91$ as fitting and $R^2 < 0.85$–$0.91 >$ as quasi fitting to the given model, although several publications also calculate with $R^2 < 0.8$ [8]. The evaluation of fit according to these criteria is summarized in Table 4.

From the data (Table 4) it can be seen that, within the tested models, none fits both considered cations simultaneously. Conversely, a common complete nonconformity can be observed to the Elovich model and almost complete nonconformity to the Dubinin-Radushkevich, where 21 kGy dosed sample for Co(II) quasi fits only.

The **Langmuir** model assumes a homogeneous single-layer adsorption where each active site has the same affinity for the adsorbate. It is generally suitable for lower adsorbate concentrations [19], probably lower than those used in our study. Although Cr(III) is of any lower concentration (12.5–70 mmol dm^{-3}) compared to Co(II) (50–200 mmol dm^{-3}), for Cr(III) this model does not fully meet any of the absorbed doses (0–410) kGy except 99 kGy quasi fitting dose as indicated (Table 2, Table 3). Ambiguous figures are shown for Co(II) (50–200 mmol dm^{-3}), where both native wool and wool dosed of 153 and 410 kGy meet the criterion; the other samples show quasi fitting except the 21 kGy dose (Table 2, Table 3). We assume the reasons for such differences are in the different ability to form a complex salt, including the intrinsic and variable architecture of the corresponding complexes. The Cr(III) cation is a weaker Lewis acid than Co(II), but the formation of Cr-complex with wool has been proven [14]. From the inadequate fitting it can be deduced that the adsorption is not fully homogeneous. Regarding the effect of electron beam, which ultimately produces other acidic groups from S-oxidized products, in particular cysteine acid R -SO$_3$H, in addition to Cr(III) carboxylate, Cr(III)-cysteinate may be formed as well. There are the double salts that can cause inhomogeneity on the wool surface. Also the structure of the respective complexes will be different, but the coordination number 6 will have to be the same. If the required number of acid groups and suitable ligands on the surface is not available for Cr(III), the adsorbate will tend to diffuse into the fiber

Table 3
The correlation equations obtained from plots for Cr(III) and Co(II) based on the linearized equations of the models presented in Table 2 for fitting or quasi fitting models only.

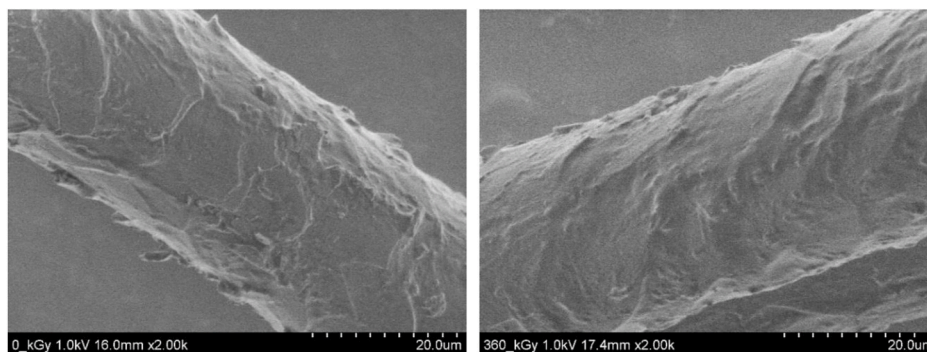| Dose	Cr(III)		Co(II)	
	Trend line equation	Correlation	Trend line equation	Correlation
(kGy)				
Langmuir				
0	$y = -0.0194x + 219.92$	$R^2 = 0.6781$	$y = 0.0663x - 114.09$	$R^2 = 0.943$
21	$y = -0.0051x + 150.32$	$R^2 = 0.0845$	$y = 0.00437x + 332.83$	$R^2 = 0.0236$
40	$y = 0.0061x + 134.78$	$R^2 = 0.1741$	$y = 0.02816x + 42.052$	$R^2 = 0.8768$
99	$y = -0.0219x + 231.2$	$R^2 = 0.8994$	$y = 0.04688x - 31.933$	$R^2 = 0.8612$
153	$y = -0.0142x + 220.03$	$R^2 = 0.5864$	$y = 0.03338x + 32.295$	$R^2 = 0.9433$
258	$y = 0.0036x + 145.54$	$R^2 = 0.3175$	$y = 0.0524x + 8.3067$	$R^2 = 0.8547$
410	$y = -0.0077x + 175.89$	$R^2 = 0.227$	$y = 0.04813x + 77.332$	$R^2 = 0.9855$
Freundlich				
0	$y = 1.3463x - 3.7612$	$R^2 = 0.8983$	$y = -0.1874x + 2.0376$	$R^2 = 0.4061$
21	$y = 1.0294x - 2.2367$	$R^2 = 0.9616$	$y = 0.2644x + 0.3446$	$R^2 = 0.7503$
40	$y = 0.8945x - 1.8244$	$R^2 = 0.9777$	$y = 0.3067x + 0.2844$	$R^2 = 0.4759$
99	$y = 1.1823x - 2.8552$	$R^2 = 0.9914$	$y = 0.1378x + 0.8504$	$R^2 = 0.099$
153	$y = 1.1036x - 2.6129$	$R^2 = 0.9877$	$y = 0.2235x + 0.557$	$R^2 = 0.5184$
258	$y = 0.9507x - 2.0243$	$R^2 = 0.9975$	$y = 0.2366x + 0.3632$	$R^2 = 0.2356$
410	$y = 1.0523x - 2.3709$	$R^2 = 0.9808$	$y = 0.2816x + 0.1379$	$R^2 = 0.8091$
Temkin				
0	$y = 11.025x - 69.812$	$R^2 = 0.8835$	$y = -3.6548x + 53.345$	$R^2 = 0.388$
21	$y = 12.799x - 80.056$	$R^2 = 0.8083$	$y = 5.4629x - 25.195$	$R^2 = 0.7284$
40	$y = 10.224x - 62.406$	$R^2 = 0.895$	$y = 7.8685x - 39.996$	$R^2 = 0.3688$
99	$y = 10.904x - 69.209$	$R^2 = 0.8862$	$y = 3.0772x - 2.6967$	$R^2 = 0.0728$
153	$y = 9.902x - 62.377$	$R^2 = 0.8953$	$y = 5.2589x - 20.24$	$R^2 = 0.4542$
258	$y = 10.192x - 62.617$	$R^2 = 0.9443$	$y = 3.8593x - 14.919$	$R^2 = 0.1571$
410	$y = 11.056x - 69.056$	$R^2 = 0.9133$	$y = 4.1583x - 20.059$	$R^2 = 0.8155$
Flory-Huggins				
0	$y = 23.873x + 0.7854$	$R^2 = 0.2373$	$y = -82.134x - 4.7179$	$R^2 = 0.9917$
21	$y = -0.8526x + 0.2421$	$R^2 = 0.0002$	$y = -67.457x - 4.5094$	$R^2 = 0.95$
40	$y = -67.738x - 1.7215$	$R^2 = 0.5169$	$y = -47.686x - 4.3317$	$R^2 = 0.8815$
99	$y = 57.177x + 1.5062$	$R^2 = 0.5813$	$y = -59.267x - 4.4818$	$R^2 = 0.8992$
153	$y = 59.779x + 1.5073$	$R^2 = 0.2838$	$y = -55.739x - 4.4226$	$R^2 = 0.9487$
258	$y = 103.3x + 2.9045$	$R^2 = 0.7014$	$y = -77.818x - 4.5889$	$R^2 = 0.8433$
410	$y = 19.877x + 0.7494$	$R^2 = 0.0332$	$y = -73.07x - 4.5493$	$R^2 = 0.9644$
Halsey				
0	$y = 1.3463x - 8.6631$	$R^2 = 0.8955$	$y = -0.1874x + 4.6918$	$R^2 = 0.4061$
21	$y = 1.029x - 5.1477$	$R^2 = 0.9613$	$y = 0.2644x + 0.7934$	$R^2 = 0.7503$
40	$y = 0.894x - 4.1963$	$R^2 = 0.9779$	$y = 0.3067x + 1.5076$	$R^2 = 0.4759$
99	$y = 1.1818x - 6.5706$	$R^2 = 0.9914$	$y = 0.1378x + 1.9579$	$R^2 = 0.099$
153	$y = 1.103x - 6.0119$	$R^2 = 0.9875$	$y = 0.2235x + 1.28242$	$R^2 = 0.5184$
258	$y = 0.9497x - 4.6533$	$R^2 = 0.9974$	$y = 0.2366x + 0.8362$	$R^2 = 0.2356$
410	$y = 1.0522x - 5.4584$	$R^2 = 0.9809$	$y = 0.2816x + 0.3175$	$R^2 = 0.8091$
Harkins-Jura				
0	$y = -0.8495x + 2.9639$	$R^2 = 0.9858$	$y = 0.0023x - 0.0065$	$R^2 = 0.4279$
21	$y = -0.0589x + 0.2053$	$R^2 = 0.9404$	$y = -0.003x + 0.0133$	$R^2 = 0.7757$
40	$y = -0.0508x + 0.1785$	$R^2 = 0.9656$	$y = -0.0023x + 0.0099$	$R^2 = 0.6667$
99	$y = -0.1456x + 0.5046$	$R^2 = 0.8826$	$y = -0.0014x + 0.0071$	$R^2 = 0.1668$
153	$y = -0.1274x + 0.4434$	$R^2 = 0.92$	$y = -0.0019x + 0.0089$	$R^2 = 0.6265$
258	$y = -0.0649x + 0.2265$	$R^2 = 0.9094$	$y = -0.0045x + 0.0203$	$R^2 = 0.4295$
410	$y = -0.0814x + 0.2839$	$R^2 = 0.948$	$y = -0.0062x + 0.0275$	$R^2 = 0.796$
Jovanovic				
0	$y = 0.0009x - 0.4059$	$R^2 = 0.9774$	$y = -4E-05x + 3.3218$	$R^2 = 0.6175$
21	$y = 0.0006x + 1.1836$	$R^2 = 0.993$	$y = 4E-05x + 2.8438$	$R^2 = 0.5746$
v40	$y = 0.0006x + 1.3163$	$R^2 = 0.9961$	$y = 4E-05x + 3.0431$	$R^2 = 0.3359$
99	$y = 0.0007x + 0.7467$	$R^2 = 0.9888$	$y = 1E-05x + 3.0991$	$R^2 = 0.0178$
153	$y = 0.0007x + 0.8241$	$R^2 = 0.9906$	$y = 3E-05x + 3.0244$	$R^2 = 0.3607$
258	$y = 0.0006x + 1.2458$	$R^2 = 0.9766$	$y = 3E-05x + 2.7295$	$R^2 = 0.1062$
410	$y = 0.0006x + 1.0513$	$R^2 = 0.9849$	$y = 4E-05x + 2.5017$	$R^2 = 0.6174$
Redlich-Peterson				
0	$y = -0.3461x + 8.6616$	$R^2 = 0.3621$	$y = 1.1874x - 2.0376$	$R^2 = 0.9648$
21	$y = -0.0288x + 5.1456$	$R^2 = 0.019$	$y = 0.7355x - 0.3446$	$R^2 = 0.9588$
40	$y = 0.1056x + 4.1994$	$R^2 = 0.3814$	$y = 0.6933x - 0.2843$	$R^2 = 0.8227$
99	$y = -0.1814x + 6.568$	$R^2 = 0.7328$	$y = 0.8622x - 0.8504$	$R^2 = 0.8113$
153	$y = -0.1029x + 6.0108$	$R^2 = 0.4085$	$y = 0.7765x - 0.557$	$R^2 = 0.9286$
258	$y = 0.0504x + 4.6527$	$R^2 = 0.5202$	$y = 0.759x - 0.3478$	$R^2 = 0.763$
410	$y = -0.0522x + 5.4579$	$R^2 = 0.1126$	$y = 0.724x - 0.1636$	$R^2 = 0.9487$

Fig. 2. SEM photos of both non-irradiated (left) and irradiated (right) sheep wool used for the adsorption experiments.

Table 4
Overview of fitting and quasi fitting selected isotherm models for Cr(III) and Co(II).

	Cr(III)		Co(II)	
Model	Fitting	Quasi fitting	Fitting	Quasi fiting
Langmuir	no	99 kGy	(0–153–410) kGy	(40–99–258) kGy
Freundlich	all except 0 kGy	0 kGy	no	no
Dubinin-Radushkevich	no	no	no	21 kGy only
Temkin	(258–410) kGy	(0–40–99–153) kGy	no	no
Flory-Huggins	no	no	(0–21–153–410) kGy	(40–99–258) kGy
Halsey	all except 0 kGy	0 kGy	No	no
Harkins-Jura	all except 99 kGy	99 kGy	no	no
Jovanovic	all	no	no	no
Elovich	no	no	no	no
Redlich-Peterson	no	no	(0–21–153–410) kGy	no

Table 5
Parameters calculated from Cr-fitting and *quasi fitting models.

|	Freundlich		Temkin		Halsey		Harkins-Jura		Jovanovic	
Dose	K_F	1/n	B	K_T	n_H	K_H	A	B	q_{max}	K_J
kGy	$(mg.g^{-1}) \cdot (mg.dm^{-3})^{1/n}$		$J.mol^{-1}$	$dm^3.g^{-1}$					$mg.g^{-1}$	$dm^3.g^{-1}$
0	*0.17	*1.36	*220.9	*1.78	*-0.74	*623.1	−1.18	- 3.49	0.67	−0.9
21	5.80	1.04	–	–	−0.97	148.8	−16.98	- 3.49	3.27	−0.6
40	14.98	0.89	*238.3	*2.23	−1.12	109.3	−19.68	- 3.51	3.73	−0.6
99	1.40	1.18	*223.4	*1.75	−0.85	259.8	*- 6.87	*- 3.47	2.11	−0.7
153	2.44	1.10	*246.0	*1.84	−1.01	440.5	- 7.85	- 3.48	2.28	−0.7
258	9.46	0.95	239.0	2.15	−1.05	134.2	- 15.41	- 3.49	3.48	−0.6
410	4.26	1.05	220.3	1.94	−0.95	179.0	- 12.28	- 3.49	2.86	−0.6
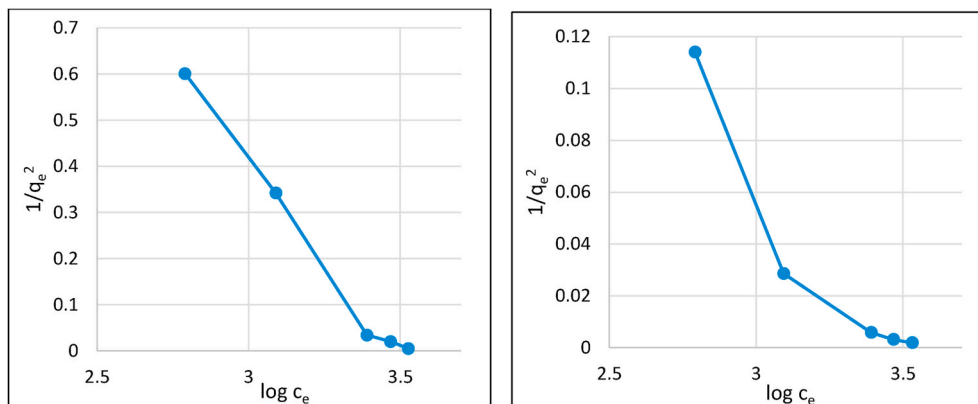
Fig. 3. Harkins-Jura plots of 0 kGy (left) and 99 kGy (right) dosed wool.

bulk and, if sterically possible, form complex salts with internal ligands.

Cobalt cation Co(II) is a stronger Lewis acid than Cr(III) and creates complex with keratin, too [13]. The variable fit rate to the Langmuir model (Table 2, Table 3) corresponds to a conception that the complex formation occurs mainly on the surface and with some structure

variability. This also corresponds to the alternation of quasi fitting with fitting. Certain exception is the 21 kGy wool showing a deviation of the R^2 value in several models. This can be explained by the fluctuation of the cystine monoxide and cystine dioxide contents, which are gradually transformed into cysteic acid [11,17] at low doses around 50 kGy dose

Table 6
Estimated equilibrium concentration of Cr(III) at the breakpoint from the Harkins-Jura plots.

Absorbed dose	log C_e at break	C_e at break
kGy		mg.dm^{-3}
0	3.42	2630
21	3.12	1318
40	3.25	1786
99	3.14	1384
153	3.18	1520
258	3.15	1409
410	3.25	1786

and the primary and secondary wool structure is complicated and especially variable.

The **Freundlich model** is not restricted to the formation of monolayer. Usually it is applied to a heterogeneous surface and to multilayer adsorption even at higher concentrations [19]. From our data (Table 3, Table 4) it is apparent that, unlike the Langmuir model, the Freundlich model is suitable for the adsorption of Cr(III) on the wool samples with all absorbed doses and only the non-irradiated wool quasi fits. In contrast to Cr(III), this model does not match Co(II) adsorption at all. On the other hand, good Cr(III) fitting indicates the fiber surface heterogeneity. Indeed, it has been found that negative charge on the surface of the natural sheep fiber is distributed non-uniformly [18], which correlates with the chemical composition [12]. The impact of the electron beam further disrupts the original chemical structure of the fiber surface enhancing the heterogeneity. The correlation equation data (Table 3) also suggest that the complex forms of Cr(III) on the surface do not form an integral barrier to further diffusion of ions into the bulk. The reason may be that, as mentioned above, Cr(III) complexes always have the coordination number of 6 and the octahedral form [15]. Therefore, the selection of ligands for Cr(III) is selective to certain extent. We assume that cations that have not found enough suitable ligands already on the surface diffuse into the fiber volume. Inside, they coordinate with suitable ligands according to spatial conditions limited by secondary structure (α-helical, β-sheet, amorphous).

The **Dubinin-Radushkevich** model is an empirical model generally applied to describe adsorption mechanism with a Gaussian energy distribution on a heterogeneous surface [19]. The model is often used to distinguish between the physical and chemical adsorption. In our case, any from the cations under consideration do not match Dubinin-Radushkevich model, indicating non-Gaussian energy distribution, except the specific 21 kGy sample for Co(II) (see Appendix). Considering the above mentioned negative charge distribution on the surface as well as double types of Cr(III)-salts (carboxylates, cysteinates), such result could be expected.

The **Temkin** model takes into account adsorbent-adsorbate interactions. The model assumes that the heat of adsorption of all molecules in the layer decreases linearly with coverage due to adsorbent-adsorbate interactions and, the binding energies are of uniform distribution [20]. The model is not too suitable for extremely high or low

concentrations. Usually application on complex adsorption system with liquid phase gives not appropriate fitting [19]. In our case the Temkin model fits the system wool-Cr(III) only partially, when the adsorption fully fits the highest dosed wool (258 kGy and 410 kGy); the lower dosed adsorbents are quasi fitting involving the native wool, too. The model matches the wool-Co(II) not at all. The reason could be the concentration higher than for Cr(III) as well as different types of the relevant complexes.

The **Flory-Huggins** model describes the degree of surface coverage characteristics of the adsorbate on the adsorbent and can express the feasibility and spontaneity of an adsorption [19]. As seen from Tables 2 and 3, the Cr(III) adsorption meets the model not at all. The Co(II) adsorption fits most of the dosed samples and the native wool shows the best result; the wool with 40 or 99 kGy are quasi fitting and the 258 kGy dosed wool is a little under the set up limit. One can say that the Co(II) adsorption approaches to fit the Flory-Huggins isotherm.

The **Halsey** model is applied on multilayer adsorption at relatively large distance from surface and the adsorbent is of heterogeneous nature [3]. The R^2 calculation for the Cr(III) sorption shows the fitting for all irradiated wool samples and quasi fitting for the native wool (Table 3, Table 4). This indicates conformity of the Cr(III) sorption to the model principles. Even only quasi fitting for the non-irradiated wool can imply a lower measure of heterogeneity compared to the exposed samples. It is remarkable that results for the Halsey model are in conformity with the Freundlich isotherm indicating the rightness of our anticipation. Also Co(II) adsorption shows the same results for the Halsey and the Freundlich models, since any sample covers the isotherm models not at all.

The **Harkins-Jura** model assumes the possibility of multilayer adsorption on the surface of adsorbent having a heterogeneous distribution of pores [13]. The prerequisities of heterogeneity and multilayer adsorption are similar to the Halsey model. Therefore, certain data similarity with that model is not surprising. Within the Harkins-Jura isotherm, all correlation data for Cr(III) excepting wool dosed 99 kGy fit and that manifests quasi fitting. The non-irradiated wool is of the highest R^2 value (Table 3). Considering the Co(II) adsorption, no the adsorbent-adsorbate system matches the Harkin-Jura isotherm (Table 3, Table 4).

In addition to the Langmuir model with monolayer adsorption without lateral interactions, the **Jovanovic** model also considers the possibility of physical binding of the adsorbate on the adsorbent surface [21]. From the cations under question only the Cr(III) adsorption on sheep wool meets the Jovanovic model fully (Table 2, Table 3) regardless absorbed dose. Besides balanced of relative rates of adsorption and desorption, this model involves some surface binding vibrations. The latter interactions could be expectable with regard to Cr(III) coordination number of 6 and an octahedral form exclusively; the fiber surface itself may not provide full saturation with needed ligands, what leads to side physical interactions, too. Different case is the Co(II) (Table 2, Table 3) since none from the samples fits the Jovanovic model at all.

The **Elovich** model assumes that the adsorption sites grow exponentially with adsorption and multilayer process occurs [20,21]. These principles are not fulfilled for any cations under examination (Table 2,

Table 7
Parameters calculated from Co-fitting and *quasi fitting models.

Dose	Langmuir				Flory-Huggins		Redlich-Peterson	
	Q	K_L	K_{FH}	n_{FH}	ΔG^0	A	β
kGy	mg.g^{-1}	dm^3.g^{-1}	dm^3.mol^{-1}		kJ.mol^{-1}	g.dm^{-3}	
0	15.08	−0.58	1.91·10^{-2}	−82.13	−26.46	1.19	0.009
21	–	–	3.09·10^{-2}	−67.46	−25.29	0.73	0.452
40	*35.54	*0.67	*4.66·10^{-2}	*-47.69 *-24.30	–	–	
99	*21.33	*-1.47	*3.30·10^{-2}	*-59.27	*-25.14	–	–
153	29.96	1.03	3.78·10^{-2}	−55.74	−24.81	0.78	0.384
258	*19.08	*6.31	*2.58·10^{-2}	*-77.82	*-25.74	–	–
410	20.78	0.62	2.82·10^{-2}	−73.07	−25.52	0.72	0.686

Table 3), what is indicated by an inadequate correlation level (see Appendix). Indeed, the adsorbed cations/complex salts on the fiber surface cannot create next adsorption points due to their binding with keratine. So that multilayer formation on the surface is out of the question.

The **Redlich-Peterson** model is a hybrid isotherm mixing the Langmuir and the Freundlich isotherms therefore does not follow ideal monolayer adsorption [19]. The model represents adsorption equilibrium over a wide concentration range applicable either on homogeneous or heterogeneous surface. That is why one could expect the adsorption fitting for all used cations. However, this supposition is not fulfilled. Testing the Cr(III) adsorption it is seen an inconvenient correlation for all dose. In the case of Co(II), most of the R^2 figures (4 from 7) matches set up criterion and, minority (3 from 7) does not match being not too far from the acceptable level.

Table 5–7 summarize the parameters calculated from the correlation equations for the fitting and quasi fitting models based on the classification predetermined.

Considering the Freundlich model, K_F represents constant indicative for relative adsorption capacity of the adsorbent [20]. The slope $1/n$ ranging between 0 and 1 is a measure of surface heterogeneity, becoming more heterogeneous as its value gets closer to zero [19]. That is not our case since all figures are far from zero (Table 5). Whereas, a value below unity should imply chemisorption process, where $1/n > 1$ is an indicative of cooperation adsorption [19]. The cooperative adsorption (or binding) occurs, when lateral interactions between molecules on the active surface play a significant role [22]. In the case of the wool, the surface provides not only carboxyl or cystein acids (main active points) to form salts with the cations but, also amino-, imino- or hydrohyl-groups. These form co-ordinative bonds giving corresponding complex salts and these present the cooperative binding. As resulting from the $1/n$ values in Table 5 and with respect to the above mentioned, the $1/n$ values oscillate around 1. That indicates each absorbed dose modifies the sorption process individually. So that we can admit certain mixed mechanism with prevalence chemisorption or cooperative adsorption following the absorbed dose. The highest $1/n$ value for the non-irradiated wool clearly indicates predominance of the cooperative adsorption. The reason is a lower amount of acid groups on the non-radiated surface than for the irradiated samples. Since the lower number of acid points the lower number of groups capable to co-ordinate is involved in the process (ligands) and, the ratio of the acid to the ligand groups is more balanced. The increase of the acid groups due to the irradiation changes that ratio.

Data for the Temkin model involve Temkin constant *b* relating to the heat of sorption and K_T is Temkin equilibrium constant [20].

According to our knowledge, physical denotation of Halsey isotherm constants n_H and K_H as well as Harkins-Jura A, B constants is not analyzed deeper in literature sources. Authors present them without any comment. In Jovanovic model the parameter q_{max} is maximum uptake of adsorbate and K_J is Jovanovic constant.

The plots of the Cr(III) dependence for the Harkins-Jura model are worth mentioning. Although approximated by a straight line, in a more detailed analysis, these show a change in the slope (similar to letter L) at a certain equilibrium concentration for all samples analyzed. As a demonstration two samples are shown in Fig. 3.

A similar observation was presented in the case of adsorption of aniline on activated charcoal and titanium dioxide from toluene; two intersecting straight lines were attributed to completion of a monolayer [23]. In our case the breakpoint could be interpreted as a qualitative change in the adsorption mechanism associated with the formation of the Cr(III)-complex on the wool surface depending on the absorbed dose. That relates with consumption of the available surface acid groups since amount of the ligands remains the same. Table 6 shows that position of the breakpoint is individual for each dose. The highest C_e for the non-irradiated wool is also associated with the highest R^2 differing from the irradiated samples (Table 3). This supports our previous findings that there are more acid groups on the surface of the irradiated samples

useable for the chemisorption of the Cr(III) cation than in the native wool [17] and, therefore less unbound cations remain in solution contacting with the irradiated samples.

The data for Co(II) (Table 7) show the fitting to the three isotherm models however, with variable level. None from the Langmuir, Flory-Huggins and Redlich-Peterson isotherms do not match Co(II)-adsorption for all dosed samples. On the other hand, the fitting and the quasi fitting samples are of similar doses. The Langmuir model assumes monolayer adsorption. If so, the monolayer should represent Co(II) complexes covered more or less the fiber surface. Since the complexes cross by more keratin chains in the fibre via the ligands, the formed network can hinder inlet the other species inside the fiber. Parameter Q represents the maximum amount of adsorbate per unit of adsorbent mass corresponding to complete coverage of adsorptive sites. The K_L is the Langmuir constant related to the energy of adsorption.

In the Flory-Huggins model, the n_{FH} is model exponent and K_{FH} is indication equilibrium of degree of surface coverage. K_{FH} is used to calculate of spontaneity free Gibbs energy following equation [19]:

$$\Delta G^0 = RT \ln K_{FH} \tag{2}$$

Tha calculated negative ΔG^0 values (Table 7) indicate spontaneous processes confirming our previous finding [13,14].

Examination of the Redlich-Peterson model shows that Co(II) adsorption achieves an adsorption equilibrium only on some dosed samples including 0 kGy. In the limit, the model approaches the Freundlich isotherm at a high concentration as exponent β tends to zero. This is the case of 0 kGy dosed wool. When β is close to one, low concentrations are concerned and the Langmuir's conditions are fulfilled [19]. Thus our data (Table 7) indicate some intermediate model from the Freundlich (the native wool) to a hybrid Freundlich-Langmuir (21–153–410 kGy) depending on absorbed dose. Recently was reported testing Cu(II) sorption for the same models under comparable conditions [16] and the copper cation showed adherence to Langmuir, Flory-Huggins and partially Redlich-Peterson models. The latter clearly distinguished the non-irradiated wool ($R^2 = 0.38$) from the modified ones ($R^2 \geq 0.9$). We attribute this similarity in the fitting to the fact that Cu(II) also shows sorptivity with some fluctuations due to several structures of the resulting complexes with keratin.

4. Conclusion

The adsorption of both Cr(III) and Co(II) cations from aqueous solutions on sheep wool native and irradiated by accelerated electron beam with the absorbed doses within (0–410) kGy was examined. The examination was focused on the fitting analysis of nine two-parameter isotherm models as Langmuir, Freundlich, Dubinin-Radushkevich, Temkin, Flory-Huggins, Halsey, Harkins-Jura, Jovanovic, Elovich and three-parameter Redlich-Peterson model. The isotherm parameters were calculated from the correlation equations describing particular graphic dependences constructed based on increasing concentrations for each cation and each absorbed doses. Classification of the related correlation coefficient R^2 based on predetermined criteria showed a different adsorption mechanism for the cations on the wool tested. Although both Cr(III) and Co(II) are Lewis acids generating complex salts as carboxylates or cysteinates with ligands from keratin, their various composition and architecture modify the adsorption differently. The chromic cation showed fitting or quasi fiting to Freundlich, Temkin, Halsey, Harkins-Jura and Jovanovic models for all dosed samples unlike cobaltous cation matching Langmuir, Flory-Huggins and Redlich-Peterson isotherm models. While Jovanovic model fits Cr(III) adsorption fully regardless dose, ful fitting of Co(II) was not observed for any model. Regarding a mixed fitting depending on dose absorbed by the wool, for Co(II) especially, the adsorption results indicate a hybrid mechanism. Therefore, it is impossible to apply a model at a flat rate regardless of the absorbed dose, cation and concentration range.

CRediT authorship contribution statement

Jana Braniša: Methodology, Formal analysis, Investigation. **Klaudia Jomová:** Funding acquisition, Resources, Project administration, Writing - review & editing. **Ľubomír Lapčík:** Formal analysis, Investigation. **Mária Porubská:** Conceptualization, Methodology, Investigation, Writing - original draft.

Declaration of competing interest

The authors declare that they have no known competing financial interests or personal relationships that could have appeared to influence the work reported in this paper.

Acknowledgement

Appendix A. Supplementary data

Supplementary data to this article can be found online at https://doi.org/10.1016/j.polymertesting.2021.107191.

References

[1] K. Wang, Y. Wu, N. Li, et al., g-Al2O3 yolk–shell porous microspheres with superior Congo red removal performance, Surf. Innov. 8 (2019), https://doi.org/10.1680/jsuin.19.00037.

[2] S.Y. Zhou, Z.Y. Yao, L.M. Qie, et al., Pb (II) adsorption by nanogoethite loaded with chestnut shell pigment, Emerg. Mater. Res. 9 (2020), https://doi.org/10.1680/jemmr.18.00123.

[3] M.T. Amin, A. Alazba, M. Shafiq, Adsorptive removal of reactive Black 5 from wastewater using bentonite clay: isotherms, kinetics and thermodynamics, Sustainability-Basel 7 (2015), https://doi.org/10.3390/su71115302.

[4] G. Nechifor, D. Pascu, M. Pascu, G.A. Traistaru, P.C. Albu, Comparative study of Temkin and Flory-Huggins isotherms for adsorption of phosphate anion on membranes, U.P.B. Sci. Bull., Ser. B: Chem. Mater. Sci. 77 (2015) 63–72.

[5] Z. Yang, Y. Chai, L. Zeng, Z. Gao, J. Zhang, H. Ji, Efficient removal of copper ion from wastewater using a stable chitosan gel material, Molecules 24 (2019), https://doi.org/10.3390/molecules24234205.

[6] S. Vilvanathan, S. Shanthakumar, Column adsorption studies on nickel and cobalt removal from aqueous solution using native and biochar form of Tectona grandis, Environ. l Prog. Sustain. 36 (2017), https://doi.org/10.1002/ep.12567.

[7] X. Chen, Modeling of experimental adsorption isotherm data, Information 6 (2015), https://doi.org/10.3390/info6010014.

[8] S. Kilpimaa, H. Runtti, T. Kangas, U. Lassi, T. Kuokkanen, Physical activation of carbon residue from biomass gasification: novel sorbent for the removal of phosphates and nitrates from aqueous solution, J. Ind. Eng. Chem. 21 (2015), https://doi.org/10.1016/j.jiec.2014.06.006.

[9] A. Ghosh, S.R. Collie, Keratinous materials as novel absorbent systems for toxic pollutants, Defence Sci. J. 64 (2014), https://doi.org/10.14429/dsj.64.7319.

[10] H.H.A. Ghafar, T. Salem, E.K. Radwan, A.A. El-Sayed, M.A. Embaby, M. Salama, Modification of waste wool fiber as low cost adsorbent for the removal of methylene blue from aqueous solution, Egypt, J. Chem. 60 (2017), https://doi.org/10.21608/ejchem.2017.687.1023.

[11] M. Porubská, Z. Hanzlíková, J. Braniša, A. Kleinová, P. Hybler, M. Fülöp, J. Ondruška, K. Jomová, The effect of electron beam on sheep wool, Polym. Degrad. Stabil. 111 (2015), https://doi.org/10.1016/j.polymdegradstab.2014.11.009.

[12] M. Porubská, A. Kleinová, P. Hybler, J. Braniša, Why natural or electron irradiated sheep wool show anomalous sorption of higher concentrations of copper(II), Molecules 23 (2018), https://doi.org/10.3390/molecules23123180.

[13] J. Braniša, K. Jomová, R. Kovalčíková, P. Hybler, M. Porubská, Role of post-exposure time in Co(II) sorption of higher concentrations on electron irradiated sheep wool, Molecules 24 (2019), https://doi.org/10.3390/molecules24142639.

[14] J. Braniša, A. Kleinová, K. Jomová, R. Malá, V. Morgunov, M. Porubská, Some properties of electron beam-irradiated sheep wool linked to Cr(III) sorption, Molecules 24 (2019), https://doi.org/10.3390/molecules24234401.

[15] J. Šima, M. Koman, A. Kotočová, P. Segľa, M. Tatarko, D. Valigura, Anorganická Chémia, second ed., STU, Bratislava, Slovakia, 2011, pp. 375–378 (in Slovak).

[16] M. Porubská, K. Jomová, Ľ. Lapčík, J. Braniša, Radiation-modified wool for adsorption of redox metals and potentially for nanoparticles, Nanotechnol. Rev. 9 (2020), https://doi.org/10.1515/ntrev-2020-0080.

[17] Z. Hanzlíková, M.K. Lawson, P. Hybler, M. Fülöp, M. Porubská, Time-dependent variations in structure of sheep wool irradiated by electron beam, Adv. Mater. Sci. Eng. (2017), https://doi.org/10.1155/2017/3849648.

[18] B. Zimmerman, J. Chow, A.G. Abbott, M.S. Ellison, M.S. Kennedy, D. Dean, Wool fibers assessed by high-resolution force spectroscopy, J. Eng. Fiber.Fabr. 6 (2011), https://doi.org/10.1177/155892501100600207.

[19] K.Y. Foo, B.H. Hameed, Insights into the modeling of adsorption isotherm systems, Chem. Eng. J. 156 (2010), https://doi.org/10.1016/j.cej.2009.09.013.

[20] O. Hamdaoui, E. Naffrechoux, Modeling of adsorption isotherms of phenol and chlorophenols onto granular activated carbon. Part I. Two-parameter models and equations allowing determination of thermodynamic parameters, J. Hazard Mater. 147 (2007), https://doi.org/10.1016/j.jhazmat.2007.01.021.

[21] R. Farouq, N.S. Yousef, Equilibrium and kinetics studies of adsorption of copper(II) ions on natural biosorbent, Int. J. Chem. Eng. Appl. 6 (2015), https://doi.org/10.7763/IJCEA.2015.V6.503.

[22] S. Liu, Cooperative adsorption on solid surfaces, J. Colloid Interface Sci. 450 (2015), https://doi.org/10.1016/j.jcis.2015.03.013.

[23] S. Shanava, A.S. Kunju, H.T. Varghese, C.Y. Panicker, Comparison on Langmuir and Harkins-Jura adsorption isotherms for the determination of surface area of solids, Orient. J. Chem. 27 (2011).